

# AN EFFECTIVE AND EFFICIENT GENERATION FRAMEWORK FOR CONDENSING THE GRAPH REPOSITORY

005 **Anonymous authors**

006 Paper under double-blind review

## ABSTRACT

011 Graph repositories with multiple graphs are increasingly prevalent in various  
 012 applications. As the amount of data increases, training neural networks on graph  
 013 repositories becomes increasingly burdensome. However, existing condensation  
 014 methods focus more on reducing the size of a single graph. They fail to address the  
 015 challenges of efficiently and effectively compressing multiple data graphs. In this  
 016 work, we propose a novel end-to-end Graph Repository Condensation (GRCOND)  
 017 framework that effectively condenses a large-scale graph repository with multiple  
 018 graphs, while preserving task-relevant structural and feature information. Unlike  
 019 traditional methods, our approach pretrains a dataset-specific GNN model to create  
 020 and optimize synthetic graphs, enabling us to capture both intra-graph structures  
 021 and inter-graph relationships, and thus providing a more holistic representation  
 022 of the repository. Through experiments, our proposed approach achieves higher  
 023 accuracy and retains features across different compression ratios, highlighting the  
 024 potential of our framework to accelerate GNN training and expand the applicability  
 025 of graph-based machine learning in resource-constrained environments.

## 1 INTRODUCTION

029 Graph repositories have become fundamental to modern data analysis across diverse domains (Gilmer  
 030 et al., 2017). From temporal network evolution analysis (Liu et al., 2021) and biological interaction  
 031 studies (Fout et al., 2017; Huang et al., 2023) to personalized recommendation systems (Fan et al.,  
 032 2019; Ying et al., 2018), such repositories encode complex relational patterns critical for advancing  
 033 scientific and industrial applications. As repositories grow in scale and complexity, training Graph  
 034 Neural Networks (GNNs) on these datasets becomes computationally prohibitive (Hamilton et al.,  
 035 2017), hindering rapid experimentation and deployment in the resource-constrained settings. As a  
 036 result, many dataset condensation methods have emerged, such as trajectory matching (Jin et al.,  
 037 2022a), distribution matching (Zhao & Bilen, 2023), and kernel-based distillation (Xu et al., 2023).  
 038 Due to the advancement of neural networks and the simplicity of image datasets, these methods  
 039 achieve effective condensation.

040 Although existing condensation methods (Gao et al., 2024; Khoshrafter & An, 2024; Dai et al., 2019)  
 041 have shown promise in reducing training costs, they predominantly focus on single-graph scenarios.  
 042 These approaches often fall short in capturing the structural diversity and inter-graph relationships  
 043 inherent in multi-graph repositories. These datasets introduce unique challenges that are not present  
 044 in single-graph settings (Tang et al., 2015; Dai et al., 2019), such as the need to preserve intergraph  
 045 relationships, structural diversity, and scalability as the dataset size grows (Velickovic et al., 2018;  
 046 Kipf & Welling, 2017; Xu et al., 2018). Therefore, *how to efficiently condense a large graph data*  
*repository into an extremely small graph data set is the main focus of our paper.*

047 To address this problem, we propose a novel graph repository condensation framework (GRCOND)  
 048 that effectively condenses a large-scale graph repository with multiple graphs. Our method can handle  
 049 the unique properties of graph repositories with multiple graphs, retaining both intra-graph and  
 050 inter-graph information, which are vital for tasks such as classification and anomaly detection.

051 To address the issue of uneven quality in small graphs within the graph repository and the high  
 052 overhead associated with directly optimizing graph data, we developed a new sample optimization  
 053 method. We first search for the cluster center for each category in the graph repository, which is the  
 054 graph with the smallest sum of distances to other samples within the category. After selecting these

representative samples, we use the pre-trained model to obtain the corresponding latent vectors, and then optimize these latent vectors during the training process.

Unlike other condensation methods, we use an end-to-end optimization approach. We trained a network to embed the node features and structural features of the graph together, and trained two decoder networks separately during restoration. This reduces the optimization overhead in the compression process without destroying the correspondence between the two, and also retains their respective characteristics. This paper makes the following four major contributions:

- We establish the first fully end-to-end condensation framework for graph repositories, unifying structural preservation and feature distillation via latent space bi-level optimization.
- We propose a framework for condensing a graph repository with multiple graphs (GRCOND), which preserves both intra-graph and inter-graph information.
- We propose a new optimization strategy in gradient matching, which utilizes a pre-trained model as the optimization tool and employs the latent vectors as optimization targets to address the discreteness problem of graph data, while also establishing an identical distribution relationship between the generated graphs.
- We conduct comprehensive experiments on various repositories and various GNNs to show the effectiveness and versatility of our proposed framework.

## 2 RELATED WORK

**Dataset Condensation.** We are witnessing an increasing number of dataset condensation techniques applied to real datasets. It works by generating a small subset of synthetic data, ensuring that it achieves similar performance to the full repository when training a deep learning model. Zhao et al. (Zhao et al., 2021a) formulate this goal as a gradient matching problem between the gradients of deep neural network weights that are trained on the original and their synthetic data. Jin et al. (Jin et al., 2022b) expand its application to graph-structured data where the samples (nodes) are interdependent. However, their methods do not apply to a graph repository with multiple graphs, which have very strong structural characteristics and strong connections between graphs. In this work, we generalize the problem of dataset condensation to the condensation of a graph repository comprising multiple graphs, and we seek a new approach to jointly learn the synthetic node features and graph structure.

**Graph Sparsification / Coarsening / Condensation.** Graph sparsification (Hashemi et al., 2024) focuses on reducing the number of edges in a graph while preserving key properties, such as pairwise distances (Peleg & Schäffer, 1989), cut values (Karger, 1994), or spectral characteristics, including eigenvalues and eigenvectors (Kipf & Welling, 2017; Spielman & Teng, 2011). In contrast, graph coarsening reduces number of nodes by aggregating original nodes into supernodes while maintaining structural and functional properties of the graph (Loukas, 2019; Loukas & Vanderghenst, 2018; Deng et al., 2020; Xu et al., 2019). This is typically achieved by defining the connections of super-nodes to approximate the behavior of the original graph, enabling efficient analysis and computation on the coarser representation (Sun et al., 2020). Among the many ways to reduce graph data storage, we are more concerned about graph repository condensation. It does not reduce the number of nodes or edges, but reduces the number of graphs, which requires paying attention to the connections between graphs while considering the connections between nodes.

## 3 PROBLEM DEFINITION

Dataset condensation is particularly relevant in scenarios requiring computational efficiency, model adaptability, and privacy-preserving machine learning solutions. It is a machine learning technique that aims at synthesizing a smaller and highly informative version of a repository.

**Definition 1 (Dataset Condensation)** *Given a large repository consisting of  $|T|$  pairs of a training object and its class label  $D_o = \{(x_i, y_i)\}_{i=1}^{|T|}$  where  $x \in X \subseteq R$ ,  $y \in \{0, \dots, C-1\}$ , the target is to learn a condensed set  $D_S$  which can train the neural network  $\phi$  on them, and this  $\phi$  can be used directly on  $Z$ .*

Dataset condensation methods primarily focus on images or tabular data, aiming to reduce the repository size without sacrificing task performance. In this paper, we will extend these techniques to

graph repositories. It introduces unique challenges due to the intricate structure of graphs, including node relationships, edge connections, and feature distributions, which must be preserved in the condensation process.

**Definition 2 (Graph,  $G$ )** A graph  $G$  is a fundamental data structure defined as a pair  $G = (V, E, X)$ , where  $V$  is a finite set of nodes, which represent the entities in the system.  $E \in V \times V$  is a set of edges that represent the relationships between the entities.  $X \in \mathbb{R}^{N \times F}$  is a matrix containing node feature information, where  $N$  and  $F$  are the number of nodes and the node features, respectively.

116 Based on the basic data structure, we will define the core issue of this paper.

**Definition 3 (Condensation for Graph Repository with Multiple Graphs)** Given a large set of graphs  $D_G = \{(G_1, y_1), (G_2, y_2), \dots, (G_N, y_N)\}$ , the goal is to condense  $D_G$  into a extremely smaller set  $D_S (|D_S| \ll |D_G|)$  such that a model trained on  $D_S$  performs similarly to a model trained on the full repository  $D_G$ . Data in  $D_S$  are all newly generated.

121 By reducing the size and complexity of graph repositories while preserving essential structural,  
122 feature, and task-specific information, condensation for a graph repository with multiple graphs  
123 enables scalable and effective downstream applications in diverse domains such as chemistry, biology,  
124 and social networks.  
125

## 4 CONDENSATION FOR GRAPH REPOSITORY

129 In this section, we introduce our proposed method for graph set condensation in detail. First, we  
130 present our overview framework. Then, we explain in turn the implementation details of each module,  
131 including explaining how to initialize model parameters, synthesize repositories, and match two  
132 repositories through the training trajectory of the same model. After that, we will demonstrate our  
133 unique approach to optimization.

## 4.1 OVERVIEW

Figure 1 shows the general framework of the condensation for the graph set. This figure consists of two parts, where the left part represents the initialization and optimization of our condensed graph repository, and the right part represents the training phase. We first use an arbitrary pretrained GNN model to learn the characteristics of the structural information of the graphs. In all our algorithm processes, the network parameters of this pretrained model will not be updated, and only its learning of structural information and generation functions will be used.

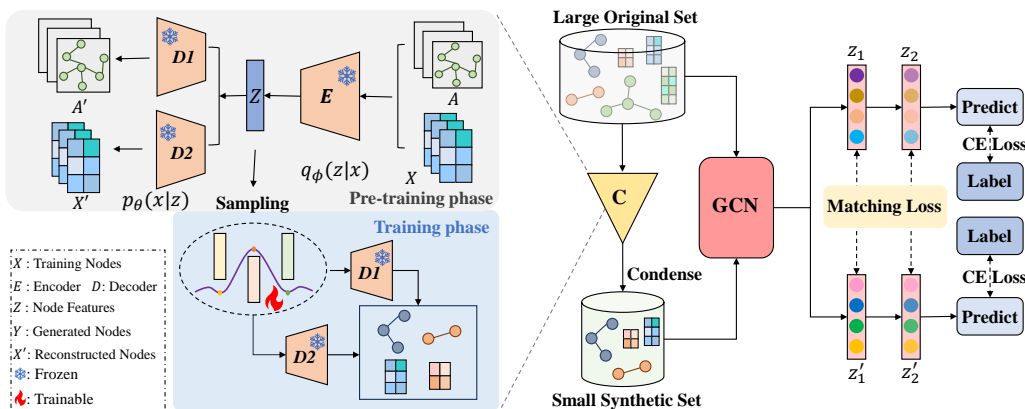


Figure 1: Framework of Condensation for Graph Repository

157 During the initialization of network parameters and synthetic repositories, we utilize the embedding  
158 part of the pre-trained model to extract the embedding matrix, which captures the representations of  
159 the graph data. Then sample the embedding vector to obtain the initial embedding of the synthetic  
160 data set. In the training phase, we employ gradient matching to align the training trajectories of the  
161 two repositories and utilize the matching loss to update the embedding vectors. Then we decode these  
vectors to restore the structure and feature information of the synthetic repository.

162 4.2 PRETRAINING  
163

164 We utilize GCN to obtain the embedding of each small graph, thereby leveraging the generalization  
165 capabilities of pre-trained GNNs to capture the structural semantics of graphs. During our formal  
166 training process, the pretrained GNN parameters are frozen and only used as a feature extractor to  
167 prevent multi-objective optimization. In the restoration stage, we pre-trained two models to decode  
168 structural features and node features, respectively, because structural features typically follow a sparse  
169 discrete distribution, and decoding requires emphasizing the locality and sparsity of topological  
170 relationships. Node features are mostly continuous, and decoding must retain semantic associations  
171 and maintain smoothness. The update process of the synthetic dataset after using the model can be  
172 expressed as follows:

$$173 S'_{t+1} = D_\psi(Z_{t+1}) = D_\psi(Z_t - \eta J_{D_\psi}(Z_t)^\top \nabla_S \mathcal{J}(S_t)), \quad (1)$$

174 where  $S'$  is the synthetic graph generated by the decoder and  $Z_t$  is the current latent variable.  $D_\psi$  is  
175 a fixed decoder.  $J_{D_\psi}(Z_t)$  is the Jacobian matrix of the decoder at  $Z_t$  and  $\eta$  is the learning rate. We  
176 then use the first-order Taylor expansion approximation:

$$178 S'_{t+1} \approx D_\psi(Z_t) - \eta J_{D_\psi}(Z_t) J_{D_\psi}(Z_t)^\top \nabla_S \mathcal{J}(S_t) \approx S_t - \eta [J_{D_\psi}(Z_t) J_{D_\psi}(Z_t)^\top] \nabla_S \mathcal{J}(S_t), \quad (2)$$

179 where  $\nabla_S \mathcal{J}(S_t)$  is the gradient of the objective function with respect to the synthetic dataset. Since  
180 the decoder remains fixed throughout the process, our approach establishes a deterministic mapping  
181 relationship. Even when employing an indirectly trained decoder, it can achieve similar results to  
182 conventional synthetic dataset optimization methods.

184 4.3 INITIALIZATION PHASE  
185

186 We sample embedding vectors from the original graphs to generate the initial embedding of the  
187 synthetic graph, and then decode them into the adjacency matrix and node features of the synthetic  
188 graph using the pre-trained model. Due to the uneven distribution of small graph quality, random  
189 sampling will result in an unstable quality of the synthetic graph. So we select cluster centers for the  
190 embedding vectors to select the most representative subgraph:

$$192 cl_i^{(t)} = \arg \min_k \left\| \mathbf{z}_i - \mathbf{m}_k^{(t)} \right\|_2^2, \quad \forall i \in \mathcal{I}_c, \quad \mathbf{m}_k^{(t+1)} = \frac{1}{|\mathcal{S}_k^{(t)}|} \sum_{i \in \mathcal{S}_k^{(t)}} \mathbf{z}_i, \quad \mathcal{S}_k^{(t)} = \left\{ i \mid cl_i^{(t)} = k \right\}, \quad (3)$$

193 where  $m_k^{(t)}$  is the centroid vector of the  $t$  round and  $k$  is the cluster ID.  $z_i$  is our embedding vectors.  
194  $cl_i^{(t)}$  is the cluster ID of the  $i$ -th vector in round  $t$ . We first assign each embedding vector to the closest  
195 cluster based on the distance, and then obtain the new cluster center by averaging the vectors within  
196 each cluster. This choice can ensure that the initialization embedding vector has high quality.

197 Then, we determine a neural network model  $GNN_{\theta_0}$  for training, where  $GNN_{\theta}$  denotes the GNN  
198 model parameterized with  $\theta$ . And  $\theta_0$  is randomly sampled from a specific distribution  $P_\theta$  to make the  
199 trained synthetic repository independent of the network's initialization parameters. After that, we can  
200 preliminarily represent our target formula. Our target is to learn an extremely small synthetic graph  
201 repository  $D_S$  such that a GNN trained on  $D_S$  can achieve great performance comparable to that of a  
202 GNN trained on the much larger original repository  $D_O$ . Thus, the objective can be formulated as the  
203 following bi-level problem:

$$204 D_S = \min_{D_S} E_{\theta_0 \sim P_\theta} [L(GNN_{\theta_S}(D_G), Y_G)] \quad s.t. \quad \theta_S = \arg \min_{\theta} L(GNN_{\theta(\theta_0)}(D_S), Y_S), \quad (4)$$

205 where  $GNN_{\theta}$  denotes the GNN model parameterized by  $\theta$ ,  $\theta_S$  denotes the parameters of the model  
206 trained on  $D_S$ , and  $L$  denotes the loss function used to measure the difference between the model's  
207 predictions and the ground truth.

213 4.4 TRAINING PHASE  
214

215 To solve the problem in equation 4, we need to make the networks trained on the two repositories  
216 closer. The goal is to find a small synthetic repository that best represents the information in the

216 original repository to make the network parameters trained by the two repositories to be similar,  
 217 which can be expressed as follows:

$$219 \quad D_S = \min_{D_S} \sum_{t=0}^{T-1} \text{Dis}(\theta_S^t, \theta_O^t) \text{ with} \quad (5)$$

$$222 \quad \theta_S^{t+1} = \Delta_\theta(L(\text{GNN}_{\theta_S^t}(D_S), Y_S)) \text{ and } \theta_O^{t+1} = \Delta_\theta(L(\text{GNN}_{\theta_O^t}(D_O), Y_O)),$$

223 so that the network trained by the synthetic graph repository can also have similar effects on the  
 224 large repository. However, the overhead of directly matching network parameters is very high, so  
 225 we choose to match the paths of training the networks of the two repositories, that is, to match the  
 226 gradients that descend during the training process.

227 Our approach does not involve solving a nested loop optimization and unrolling the entire training  
 228 trajectory of the inner problem, which can be prohibitively expensive. Instead, we follow the gradient  
 229 matching method proposed in (Zhao et al., 2021b), which aims to match the network parameters  
 230 between large-real and small-synthetic training data by matching their gradients at each training step:

$$232 \quad \nabla_\theta L(\text{GNN}_{\theta^t}(D), Y) = (\theta^{t+1} - \theta^t) / \mu, \quad (6)$$

233 where  $\nabla$  is the gradient of the network’s descent at the corresponding step, and  $\mu$  is the learning rate.  
 234 In this way, the training trajectory on the small synthetic graph repository  $D_S$  can mimic that on the  
 235 large real graph repository  $D_O$ . The gradients matching process for GNN can be modeled as follows:

$$237 \quad \min_{D_S} \sum_{t=0}^{T-1} \text{Dis}(\nabla_{D_S}^t, \nabla_{D_O}^t), \quad (7)$$

240 where  $\nabla_{D_S}^t$  represents the gradient of the repository  $D_S$  at the  $t$  step of the network, and  $\text{Dis}$  is a  
 241 function that calculates the distance between two gradients. To more accurately match the training  
 242 gradients between the synthetic dataset and the original dataset, we performed a gradient matching  
 243 operation on each class, allowing the synthetic repository to learn the differences between classes.  
 244 Additionally, as demonstrated in the work on reconstructing data from gradients, large batch sizes  
 245 tend to make reconstruction more challenging. We sample a fixed-size set of neighbors on the original  
 246 graph in each training round, employing a mini-batch training strategy.

247 This phase helps preserve the inter-graph information. We use gradient matching to optimize em-  
 248 bedding parameters, ensuring that synthetic data produces model update directions equivalent to  
 249 those of the original data in downstream task training. For example, during the training of a graph  
 250 classification task, the embedding vectors corresponding to graphs of the same category are adjusted  
 251 to conform to a similar distribution, while the distance between graphs of different categories is  
 252 increased. In this way, the synthetic dataset can learn the relationship between graphs.

#### 253 4.5 OPTIMIZATION OF CONDENSED GRAPH REPOSITORY

255 We calculate the distance between the gradients of the two repositories obtained in the model  
 256 training as the loss value. Then, the goal of optimization needs to be considered. For repositories  
 257 with multiple graphs, we use our pretrained decoders to optimize synthetic repositories. Since  
 258 repositories with multiple graphs generally conform to a specific distribution and exhibit distinct  
 259 characteristics in their graph structure, such as those found in molecular, biological, and chem-  
 260 informatics repositories. The pre-trained GNN model  $\phi_{gen}$  will learn the distribution of the graph  
 261 structures in the repository, meaning that the graphs generated by the model essentially conform to  
 262 the distribution of the corresponding repository. The resulting graph will contain more information  
 263 about the original repository and facilitate our optimization work. In our work, the optimization target  
 264 is the latent vector in the graph generation model, specifically a set of latent vectors sampled during  
 265 the initialization phase. The purpose is to transform the discrete adjacency matrix into a continuous  
 266 embedding, which can be expressed as follows:

$$267 \quad Z^{t+1} = Z^t - \nabla_Z \text{Dis}(\nabla_{\text{GNN}_{D_S}}^t, \nabla_{\text{GNN}_{D_O}}^t), \quad (8)$$

268 where  $Z^t$  is the hidden vector at the  $t$ -th round of training, and  $\nabla_Z$  is the gradient calculated for each  
 269 position of  $Z$  using the loss value generated by gradient matching to optimize the hidden vector. We

270 can achieve better results by performing gradient descent on the loss value on continuous data. Then,  
 271 the latent vector after gradient descent is converted into an adjacency matrix using the decoding part  
 272 of the trained graph generation model.

273

$$274 \quad A_g = \phi_{gen}(Z_g), \\ 275 \quad A_g^{(k)}_{(i,j)} = \psi \left( \alpha \cdot f^{(k)}(Z_g, i) + \beta \cdot f^{(k)}(Z_g, j) \right), \\ 276 \quad f^{(k)}(Z_g, i) = \sigma \left( W^{(k)} Z_g^{(k-1)} \right), \\ 277 \quad 278$$

279 where  $A_g$  is the adjacency matrix corresponding to the  $g^{th}$  graph.  $\sigma$  and  $\psi$  are the activation function  
 280 of pretrained GNN model and  $W$  is pretrained parameters. Since the decoder part of the graph  
 281 generation model  $\phi_{gen}$  has been trained to generate graphs that conform to the distribution, its  
 282 parameters will not change during the whole process to ensure that the reconstructed graph also  
 283 contains the intra-graph information learned from the pretraining phase.

284 **4.6 IMPLEMENTATION**

285 Algorithm 1 shows the overall process of  
 286 condensation for the graph repository. In lines 1-2,  
 287 the original dataset and pretrained model are  
 288 given. Line 4 is the initialization phase of the  
 289 synthetic graph, where we sample embedding  
 290 vectors by Equation equation 3. Lines 7-8 calculate  
 291 the loss value of the two datasets on the  
 292 downstream task. Line 9 calculates the differ-  
 293 ence between the descent gradient of the syn-  
 294 thetic dataset and the original dataset. Lines 10-  
 295 12 optimize the embedding vector based on the  
 296 loss value and utilize the pre-trained decoder to  
 297 update the synthetic dataset. Line 13 uses the  
 298 loss value of the original dataset to optimize the  
 299 model for downstream tasks.

300 **5 EXPERIMENT**

301 To evaluate the effectiveness of our approach,  
 302 we implemented our framework on top of Py-  
 303 torch (version 2.5.0). All experiments were car-  
 304 ried out on a workstation with an Ubuntu oper-  
 305 ating system, an Intel i9-12900K CPU, 128GB  
 306 of memory, and a NVIDIA GeForce GTX4090  
 307 GPU. In this section, we designed comprehen-  
 308 sive experiments to answer the following three  
 309 research questions (RQs).

310 **RQ1 (Superiority)** What are the advantages of GRCOND compared with state-of-the-art methods?

311 **RQ2 (Effectiveness)** Can our method effectively condense the repository so that the compressed data  
 312 set has a similar effect to the original repository?

313 **RQ3 (Module necessity)** Does each of our modules play its own role and promote the results?

314 **RQ4 (Meaningfulness)** Can our condensed graphs show the original graph repository's properties?

315 **5.1 EXPERIMENTAL SETTINGS**

316 **Datasets.** In this paper, we selected five real-world graph classification datasets, including NCI1, DD  
 317 from TUDataset (Morris et al., 2020), and ogbg-molhiv, ogbg-molbbp, and ogbg-molbace from the  
 318 Open Graph Benchmarks (Hu et al., 2020). Table 1 presents the detailed statistics of the dataset. For  
 319 these datasets, 80/10/10% of the graphs are randomly split into training/validation/test sets.

320 **Baselines.** To comprehensively evaluate the performance of our condensation method for the graph  
 321 repository using the multiple graphs approach, we compared it against a diverse set of baselines,

**Algorithm 1: Our Condensation Algorithm**

---

1 **Input:** Training graph set  
 $D_G = \{G_1, G_2, \dots, G_N\}$ , number of  
 outer-loop steps  $K$ , randomly initialized  
 weights  $P_{\theta_0}$ , number of inner-loop steps  $T$ ,  
 number of classes  $C$ , GNN  $\phi_{\theta}$ , loss function  $\ell$   
 for the graph classification, pre-trained GNN  
 model  $\phi_{gen}$ .

2 **Output:** Condensed graph set  
 $D_S = \{G_1, G_2, \dots, G_M\}$ , where  $M \ll N$  and  
 $D_S \not\subseteq D_G$ .

3 **for**  $k = 0, \dots, K - 1$  **do**

4   sample  $\theta_0 \sim P_{\theta_0}$  and  $Z_{D_S} \sim P_Z$ ;

5   **for**  $t = 0, \dots, T - 1$  **do**

6     **for**  $c = 0, \dots, C - 1$  **do**

7       Sample  $B_c^{D_G} \sim D_G$ ;

8       Compute

9        $L_{D_G} = \ell(\phi_{\theta_t}(B_c^{D_G}), Y)$ ,  
 $L_{D_S} = \ell(\phi_{\theta_t}(A_{D_S}, X_{D_S}), Y)$ ;

10       Compute

11        $L_g \leftarrow D(\nabla L_{D_G}, \nabla L_{D_S})$ ;

12       Update

13        $Z_{D_S} \leftarrow Z_{D_S} - \eta \cdot \nabla L_g(Z_{D_S})$ ;

14     **end**

15     Update  $A_{D_S}, X_{D_S} \leftarrow \phi_{gen}(Z_{D_S})$ ;

16      $\theta_{t+1} \leftarrow opt_{\theta}(L_{D_G})$ ;

17 **end**

18 **return**  $D_S$

---

324  
325  
326  
327  
328  
329  
330  
331  
332  
333  
334  
335  
336  
337  
338  
339  
340  
341  
342  
343  
344  
345  
346  
347  
348  
349  
350  
351  
352  
353  
354  
355  
356  
357  
358  
359  
360  
361  
362  
363  
364  
365  
366  
367  
368  
369  
370  
371  
372  
373  
374  
375  
376  
377  
Table 1: Statistics of the tested real-world graph repositories.

Dataset	Type	# of Graphs	# of Avg. Nodes	# of Avg. Edges	# of Attributes	# of Classes
NCII	Chemical	4110	110	64	37	2
DD	Bioinformatics	1179	284	14322	89	2
ogbg-molhiv	Bioinformatics	41127	25.5	27.5	9	2
ogbg-molbbp	Bioinformatics	2,039	24	26	9	2
ogbg-molbace	Bioinformatics	1,513	34.1	36.9	9	2

including state-of-the-art approaches in graph dataset condensation and sampling. The baselines are categorized as follows. For the condensation methods, we selected representative methods from each classic compression type. DosCond (Jin et al., 2022a) is a graph dataset condensation method based on gradient matching. KiDD (Xu et al., 2023) is based on kernel ridge regression, which utilizes the graph neural tangent kernel instead of optimizing the neural network; however, its computational overhead can be very high for large datasets. Mirage (Gupta et al., 2024) extracts frequent computational tree patterns, thereby reducing the size of the training data while maintaining model performance. However, for non-message passing architectures, Mirage may not be applicable or perform poorly. Meanwhile, we also selected some simple baselines, such as full data training, random subsampling, and k-center. Full data training means training GNNs on the original multi-graph dataset without any condensation. This serves as an upper bound for task performance. Random subsampling involves randomly selecting a subset of graphs or nodes within graphs to create a condensed repository. K-Center selects k center points from the given sample set so that their distances to all samples are minimized. Although naive, this baseline highlights value of task-informed condensation methods.

**Hyperparameter Settings.** We set the hyperparameters for the proposed condensation method on a graph repository using the multiple graphs approach and the baseline approaches. The key hyperparameter settings used in our experiments are summarized below. For the condensation method, the number of condensed graphs was set to 1, 5, 10, 20, and 50 per class. The learning rates for structure and feature are set to 0.001 and 0.0001, respectively, and the Adam optimizer with a weight decay of  $5 \times 10^{-4}$  was used. In the evaluation stage, we train the same network for 1,000 epochs on the condensed graph with a learning rate of 0.001.

## 5.2 COMPARISON WITH STATE-OF-THE-ARTS (RQ1)

To demonstrate the superiority of our method, we conducted comprehensive comparative experiments on graph classification tasks to evaluate the performance of our proposed method against other graph repository condensation approaches and sampling. Table 2 presents the detailed comparison results. Column 1 lists the names of five widely used repositories for graph classification, ensuring a diverse range of benchmarks. Column 2 provides the condensation rate for each repository, representing the proportion of the original graph data retained after applying the respective condensation method. Columns 3-8 show the test accuracy achieved using four graph condensation techniques, including our proposed method, under identical condensation rates. Column 9 reports the test accuracy of the original repositories without any condensation, serving as an upper-bound reference for performance.

From this Table, we can see that GRCOND not only condenses the repository effectively but also has the lowest information loss rate. It can achieve a recurrence rate of at least 81.67% in accuracy, even when there is only one graph in each class, and achieve a recurrence rate of up to 98.27% when there are 50 graphs per class. The results demonstrate that, under the same compression rate, the repositories condensed using our method consistently achieve superior test accuracy compared to other methods. This highlights the superiority of our approach in preserving critical information for downstream tasks. Specifically, our method outperforms sampling and repository condensation significantly. The superior performance of our method can be attributed to its ability to jointly preserve structural, feature, and task-specific information across multiple graphs. Unlike traditional methods that focus solely on sparsity or coarsening, our approach optimally condenses the relevant information for downstream tasks, leading to better generalization and reduced computational overhead.

## 5.3 TEST WITH DIFFERENT GNNs (RQ2)

To evaluate the effectiveness of the proposed condensation method for the graph repository with multiple graphs, we performed experiments using various GNN architectures. These experiments were designed to assess whether the condensed graphs generated by our method are compatible

Table 2: Comparison of different baselines and GRCOND on various repositories with attributes. The best performance is **highlighted** in bold.

Dataset	GPC	Methods						Whole Dataset
		Random	K-Center	DosCond	KiDD	Mirage	GRCOND	
NCII (ACC)	1	50.90±2.10	51.90±1.60	49.20±1.10	60.40±0.50	50.80±2.20	<b>60.64±2.56</b>	80.0±1.8
	5	52.10±1.00	47.00±1.10	51.10±0.80	63.20±0.20	51.30±1.10	<b>64.54±1.74</b>	
	10	55.60±1.90	49.40±1.80	50.30±1.30	64.20±0.10	51.70±1.40	<b>64.90±1.56</b>	
	20	58.70±1.40	55.20±1.60	50.30±1.30	60.90±0.70	52.10±2.20	<b>65.53±2.46</b>	
	50	61.10±1.20	62.70±1.50	50.30±1.30	65.40±0.60	52.40±2.70	<b>69.09±1.16</b>	
DD (ACC)	1	49.70±1.30	58.80±6.10	46.30±8.50	71.30±1.50	<b>74.00±0.40</b>	69.88±0.84	76.9±2.2
	5	40.80±4.30	51.30±5.30	57.50±5.60	70.90±1.10	-	<b>71.28±0.64</b>	
	10	63.10±5.20	53.40±3.10	46.30±8.50	71.50±0.50	-	<b>72.49±1.56</b>	
	20	56.40±4.30	58.50±5.70	40.70±0.00	71.20±0.90	-	<b>71.33±1.92</b>	
	50	58.90±6.30	62.30±2.50	44.00±6.70	71.80±1.00	-	<b>73.27±3.24</b>	
ogbg-molhiv (ROC-AUC)	1	0.366±.087	0.462±.072	0.674±.131	0.664±.016	<b>0.710±.009</b>	0.644±.007	0.701±.028
	5	0.501±.051	0.519±.096	0.369±.175	0.657±.005	0.703±.012	<b>0.715±.015</b>	
	10	0.554±.031	0.471±.054	0.457±.214	0.632±.000	0.513±.055	<b>0.646±.009</b>	
	20	0.621±.022	0.627±.050	0.281±.007	0.648±.025	0.633±.048	<b>0.669±.012</b>	
	50	0.625±.062	0.680±.049	0.455±.214	0.587±.038	0.588±.067	<b>0.688±.014</b>	
ogbg_molbace (ROC-AUC)	1	0.468±.045	0.486±.035	0.512±.092	0.706±.000	0.590±.004	<b>0.710±.041</b>	0.763±.020
	5	0.312±.019	0.553±.024	0.555±.079	0.562±.000	0.419±.010	<b>0.671±.035</b>	
	10	0.442±.028	0.594±.019	0.536±.072	0.594±.000	0.419±.010	<b>0.674±.028</b>	
	20	0.510±.023	0.512±.031	0.484±.080	0.640±.011	0.423±.011	<b>0.643±.036</b>	
	50	0.486±.020	0.595±.026	0.503±.084	0.723±.011	-	<b>0.681±.024</b>	
ogbg_molbbbp (ROC-AUC)	1	0.510±.013	0.532±.015	0.546±.026	0.616±.000	0.592±.004	<b>0.627±.043</b>	0.635±.017
	5	0.522±.014	0.581±.022	0.519±.041	0.607±.005	0.431±.013	<b>0.620±.033</b>	
	10	0.508±.018	0.619±.027	0.505±.028	<b>0.663±.000</b>	0.465±.036	0.656±.029	
	20	0.567±.010	0.546±.012	0.493±.031	0.677±.001	0.610±.022	<b>0.680±.015</b>	
	50	0.595±.014	0.594±.016	0.509±.015	<b>0.684±.009</b>	0.590±.031	0.678±.024	

with different GNN models and can maintain high performance across a range of architectures. Additionally, we aimed to examine the transferability of task-specific information preserved in the condensed graphs by testing their performance on unseen GNN architectures. Row 3-7 in Table 3 summarizes the test accuracy results for synthetic repositories trained with one GNN and tested with different networks. The first column lists the GNN models used for training on the condensed repositories (e.g., GCN, GAT, and GraphSAGE), while Columns 2-6 present the test accuracy results for other GNNs when applied to the same task on the condensed repositories. The results demonstrate that condensed repositories consistently deliver high performance across a range of test networks, underscoring the compatibility of our method with diverse GNN architectures. To further highlight the impact of condensation, Row 2 in Table 3 compares the accuracy of each GNN on the complete uncondensed repository. Our condensation method retains information in the original graph repository by comparing the test accuracy on the original repository with that on the condensed repository.

From Table 3, we can see that the repository condensed by DGCNN can be effectively used to train the remaining networks, achieving a test accuracy restoration effect of at least 92.80%. A repository condensed by other methods can also achieve an 87.73% restoration effect in training neural networks. Furthermore, the results reveal that regardless of the GNN used for condensation, the test accuracy of a given network differs by up to 4.33%. This highlights the robustness and effectiveness of the condensed graphs. By preserving task-relevant information, synthetic graphs facilitate effective training and testing across a diverse set of GNN models, making them a valuable tool for reducing repository size without sacrificing performance.

Table 3: Cross-architecture performance in accuracy (%) for condensed 5 graphs/class (with a condensation rate of 1%) in PROTEINS repository

Test/Train	DGCNN	GIN	GAT	GraphSAGE	GCN
Full Test	74.10 $\pm$ 0.57	66.07 $\pm$ 0.92	65.17 $\pm$ 0.63	66.96 $\pm$ 0.78	61.60 $\pm$ 0.84
DGCNN	71.61 $\pm$ 0.73	62.50 $\pm$ 0.41	61.42 $\pm$ 1.63	62.14 $\pm$ 1.18	60.72 $\pm$ 1.29
GIN	68.07 $\pm$ 0.76	59.52 $\pm$ 1.06	60.73 $\pm$ 0.98	59.52 $\pm$ 0.85	58.54 $\pm$ 1.57
GAT	72.03 $\pm$ 0.69	58.17 $\pm$ 0.91	60.71 $\pm$ 1.67	60.39 $\pm$ 0.53	59.46 $\pm$ 0.82
GraphSAGE	69.17 $\pm$ 0.90	61.30 $\pm$ 0.78	61.01 $\pm$ 0.81	62.04 $\pm$ 2.14	58.92 $\pm$ 2.05
GCN	69.04 $\pm$ 1.40	60.82 $\pm$ 1.35	59.22 $\pm$ 1.29	58.75 $\pm$ 0.79	59.64 $\pm$ 0.94

## 5.4 ABLATION STUDY (RQ3)

To demonstrate the necessity of GRCOND in each main module, we tested various variants of GRCOND to conduct ablation experiments. The results are presented in Table 4, which describes the experiments designed for two modules. For the pretrained model, we designed two variants: one variant excluded the complete pre-trained model. We directly perform gradient descent on the node features and structural features of the graph to optimize graph data. The other variant used the

432 untrained model to test, demonstrating that even if the pre-trained model is average, it can achieve  
 433 results similar to those of conventional synthetic dataset optimization methods.  
 434

435 For our optimization module, we designed three specific variants: one variant excludes the optimization  
 436 operation for the adjacency matrix, another removes the optimization operation for node features,  
 437 and the third eliminates both optimization components. In the second column of the table, we use  
 438 three different evaluation indicators to describe the test results specifically. The second row enumerates  
 439 these variants and GRCOND. Rows 3 and 5 are the accuracy (ACC) of the prediction results.  
 440 Rows 4 and 6 are the Jaccard scores (JAC) of the predicted results, which is a metric that measures  
 441 the similarity between two sets, particularly useful for multi-label classification and segmentation  
 442 tasks. Rows 5 and 7 are the macro f1-scores (MF1), which are an aggregate metric that considers  
 443 precision and recall across all classes, treating each class equally regardless of its size. From Table 4,  
 444 GRCOND consistently outperforms its variant models, achieving up to a 16.54% gain in accuracy and  
 445 a 22.33% improvement in Jaccard score, indicating that GRCOND’s operation in the optimization  
 446 part is reasonable and effective.

446 Table 4: Performance of the variants on PROTEINS and NCI1

Dataset	Metric	Variant				
		w/o VAE	untrained VAE	pretrained VAE	w/o opt(A)	w/o opt(X)
PROTEINS	ACC	67.55±0.71	67.07±0.85	71.61±0.73	68.75±1.73	66.85±1.65
	JAC	51.29±1.51	51.16±1.82	59.61±1.05	46.77±1.96	44.77±2.13
	MF1	67.24±1.36	67.31±1.15	73.40±1.52	68.60±1.82	66.96±1.55
NCI1	ACC	61.42±1.25	61.45±1.72	69.09±1.16	63.78±1.88	60.82±2.21
	JAC	45.83±1.47	45.69±0.97	51.58±1.02	42.96±1.54	44.09±3.13
	MF1	59.01±1.24	60.73±1.43	68.24±0.89	61.31±1.35	59.90±2.53

## 454 5.5 VISUALIZATION (RQ4)

455 To intuitively demonstrate the meaning-  
 456 fulness of our proposed condensation for  
 457 the graph repository with multiple graphs  
 458 method, we provide visualizations com-  
 459 paring the original and condensed graphs.  
 460 These visualizations utilize colors to rep-  
 461 resent specific labels. Such visualizations  
 462 aim to illustrate how our method suc-  
 463 cessfully retains critical structural and feature  
 464 information even after significant conden-  
 465 sation. In Figure 2, we compare a subset  
 466 of our synthetic repository (on the left)  
 467 with a corresponding portion of the orig-  
 468 inal repository (on the right). The visual  
 469 differences between the two classes are  
 470 evident in the graphs. For instance, the blue  
 471 class exhibits a more divergent structure with  
 472 fewer loops, while the red class demon-  
 473 strates a tighter configuration with more  
 474 loops. These distinctions are key to  
 475 class differentiation and are effectively  
 476 preserved in the synthetic repository. In  
 477 particular, our method not only replicates  
 478 the original graph but also generates a  
 479 condensed version that retains these crucial  
 480 structural patterns. This ability to maintain  
 481 the defining characteristics of the original  
 482 graphs, while significantly reducing the  
 483 repository size, underscores the effectiveness  
 484 of our proposed approach.

## 485 6 CONCLUSION

486 In this paper, we present a novel graph condensation framework that effectively condenses large-scale  
 487 graph datasets into compact synthetic sets while preserving critical structural and semantic infor-  
 488 mation. The proposed algorithm ensures that synthetic graphs not only mimic the statistical properties  
 489 of the original data but also replicate the training dynamics of graph neural networks (GNNs). The  
 490 proposed method addresses limitations of conventional dataset condensation techniques, which often  
 491 fail to handle graph-structured data or rely solely on output-space matching. Experimental validation  
 492 demonstrates its superiority over random sampling, coresnet selection, and graph-level condensation  
 493 baselines in terms of classification accuracy and structural preservation. Future directions may explore  
 494 advanced pretrained graph models and extensions to dynamic or heterogeneous graphs.

486 REFERENCES  
487

488 Hanjun Dai, Yujia Li, Chenglong Wang, Rishabh Singh, Po-Sen Huang, and Pushmeet Kohli. Learning  
489 transferable graph exploration. In *Proceedings of Annual Conference on Neural Information  
490 Processing Systems (NeurIPS)*, 8-14, pp. 2514–2525, 2019.

491 Chenhui Deng, Zhiqiang Zhao, Yongyu Wang, Zhiru Zhang, and Zhuo Feng. Graphzoom: A multi-  
492 level spectral approach for accurate and scalable graph embedding. In *International Conference on  
493 Learning Representations (ICLR)*, 2020.

494 Wenqi Fan, Yao Ma, Qing Li, Yuan He, Yihong Eric Zhao, Jiliang Tang, and Dawei Yin. Graph  
495 neural networks for social recommendation. In *The World Wide Web Conference (WWW)*, pp.  
496 417–426, 2019.

497 Alex Fout, Jonathon Byrd, Basir Shariat, and Asa Ben-Hur. Protein interface prediction using graph  
498 convolutional networks. In *Proceedings of Annual Conference on Neural Information Processing  
499 (NeurIPS)*, pp. 6530–6539, 2017.

500 Xinyi Gao, Tong Chen, Yilong Zang, Wentao Zhang, Quoc Viet Hung Nguyen, Kai Zheng, and  
501 Hongzhi Yin. Graph condensation for inductive node representation learning. In *IEEE International  
502 Conference on Data Engineering (ICDE)*, pp. 3056–3069. IEEE, 2024.

503 Justin Gilmer, Samuel S. Schoenholz, Patrick F. Riley, Oriol Vinyals, and George E. Dahl. Neural  
504 message passing for quantum chemistry. In *Proceedings of International Conference on Machine  
505 Learning (ICML)*, volume 70, pp. 1263–1272, 2017.

506 Mridul Gupta, Sahil Manchanda, Hariprasad Kodamana, and Sayan Ranu. Mirage: Model-agnostic  
507 graph distillation for graph classification. In *The Twelfth International Conference on Learning  
508 Representations (ICLR)*, 2024.

509 William L. Hamilton, Zhitao Ying, and Jure Leskovec. Inductive representation learning on large  
510 graphs. In *Proceedings of Annual Conference on Neural Information Processing Systems (NeurIPS)*,  
511 pp. 1024–1034, 2017.

512 Mohammad Hashemi, Shengbo Gong, Junlong Ni, Wenqi Fan, B Aditya Prakash, and Wei Jin. A com-  
513 prehensive survey on graph reduction: Sparsification, coarsening, and condensation. *International  
514 Joint Conference on Artificial Intelligence (IJCAI)*, 2024.

515 Weihua Hu, Matthias Fey, Marinka Zitnik, Yuxiao Dong, Hongyu Ren, Bowen Liu, Michele Catasta,  
516 and Jure Leskovec. Open graph benchmark: Datasets for machine learning on graphs. In *Annual  
517 Conference on Neural Information Processing Systems (NeurIPS)*, 2020.

518 Tzu-Chen Huang, Te-Cheng Hsu, Yi-Hsien Hsieh, and Che Lin. Utilizing graph neural networks  
519 for breast cancer prognosis prediction with high-dimensional genomic data. In *International  
520 Conference of the IEEE Engineering in Medicine & Biology Society (EMBC)*, pp. 1–4, 2023.

521 Wei Jin, Xianfeng Tang, Haoming Jiang, Zheng Li, Danqing Zhang, Jiliang Tang, and Bing Yin.  
522 Condensing graphs via one-step gradient matching. In *The 28th ACM SIGKDD Conference on  
523 Knowledge Discovery and Data Mining (KDD)*, pp. 720–730, 2022a.

524 Wei Jin, Lingxiao Zhao, Shichang Zhang, Yozhen Liu, Jiliang Tang, and Neil Shah. Graph condensation  
525 for graph neural networks. In *International Conference on Learning Representations (ICLR)*,  
526 2022b.

527 David R. Karger. Random sampling in cut, flow, and network design problems. *ACM Symposium on  
528 Theory of Computing (STOC)*, 1994.

529 Shima Khoshraftar and Aijun An. A survey on graph representation learning methods. *ACM  
530 Transactions on Intelligent Systems and Technology (TSIT)*, 15(1):19:1–19:55, 2024. doi: 10.1145/  
531 3633518.

532 Thomas N. Kipf and Max Welling. Semi-supervised classification with graph convolutional networks.  
533 In *International Conference on Learning Representations (ICLR)*, 2017.

540 Xiaorui Liu, Wei Jin, Yao Ma, Yaxin Li, Hua Liu, Yiqi Wang, Ming Yan, and Jiliang Tang. Elastic  
 541 graph neural networks. In *Proceedings of International Conference on Machine Learning (ICML)*,  
 542 volume 139, pp. 6837–6849, 2021.

543 Andreas Loukas. Graph reduction with spectral and cut guarantees. *Journal of Machine Learning  
 544 Research*, 20:116:1–116:42, 2019.

545 Andreas Loukas and Pierre Vandergheynst. Spectrally approximating large graphs with smaller  
 546 graphs. In *International Conference on Machine Learning (ICML)*, pp. 3243–3252, 2018.

547 Christopher Morris, Nils M. Kriege, Franka Bause, Kristian Kersting, Petra Mutzel, and Marion  
 548 Neumann. Tudataset: A collection of benchmark datasets for learning with graphs. *arXiv preprint  
 549 arXiv:2007.08663*, 2020.

550 David Peleg and Alejandro A. Schäffer. Graph spanners. *Journal of Graph Theory*, 13(1):99–116,  
 551 1989.

552 Daniel A. Spielman and Shang-Hua Teng. Spectral sparsification of graphs. *Siam Journal On  
 553 Scientific Computing*, 40(4):981–1025, 2011.

554 Fan-Yun Sun, Jordan Hoffmann, Vikas Verma, and Jian Tang. Infograph: Unsupervised and semi-  
 555 supervised graph-level representation learning via mutual information maximization. In *Interna-  
 556 tional Conference on Learning Representations (ICLR)*, 2020.

557 Jian Tang, Meng Qu, Mingzhe Wang, Ming Zhang, Jun Yan, and Qiaozhu Mei. LINE: large-scale  
 558 information network embedding. In *Proceedings of the 24th International Conference on World  
 559 Wide Web (WWW)*, pp. 1067–1077, 2015.

560 Petar Velickovic, Guillem Cucurull, Arantxa Casanova, Adriana Romero, Pietro Liò, and Yoshua  
 561 Bengio. Graph attention networks. In *International Conference on Learning Representations  
 562 (ICLR)*, 2018.

563 Keyulu Xu, Chengtao Li, Yonglong Tian, Tomohiro Sonobe, Ken-ichi Kawarabayashi, and Stefanie  
 564 Jegelka. Representation learning on graphs with jumping knowledge networks. In *Proceedings of  
 565 International Conference on Machine Learning (ICML)*, volume 80, pp. 5449–5458, 2018.

566 Keyulu Xu, Weihua Hu, Jure Leskovec, and Stefanie Jegelka. How powerful are graph neural  
 567 networks? In *International Conference on Learning Representations (ICLR)*, 2019.

568 Zhe Xu, Yuzhong Chen, Menghai Pan, Huiyuan Chen, Mahashweta Das, Hao Yang, and Hanghang  
 569 Tong. Kernel ridge regression-based graph dataset distillation. In *Proceedings of the 29th ACM  
 570 SIGKDD Conference on Knowledge Discovery and Data Mining (KDD)*, pp. 2850–2861, 2023.

571 Rex Ying, Ruining He, Kaifeng Chen, Pong Eksombatchai, William L. Hamilton, and Jure Leskovec.  
 572 Graph convolutional neural networks for web-scale recommender systems. In *Proceedings of  
 573 International Conference on Knowledge Discovery & Data Mining (KDD)*, pp. 974–983, 2018.

574 Bo Zhao and Hakan Bilen. Dataset condensation with distribution matching. 2023.

575 Bo Zhao, Konda Reddy Mopuri, and Hakan Bilen. Dataset condensation with gradient matching. In  
 576 *International Conference on Learning Representations (ICLR)*, 2021a.

577 Jianan Zhao, Xiao Wang, Chuan Shi, Binbin Hu, Guojie Song, and Yanfang Ye. Heterogeneous graph  
 578 structure learning for graph neural networks. In *AAAI Conference on Artificial Intelligence (AAAI)*,  
 579 pp. 4697–4705, 2021b.

580  
 581  
 582  
 583  
 584  
 585  
 586  
 587  
 588  
 589  
 590  
 591  
 592  
 593

594 **A COMSUPTION ANALYSIS**

595

596 We have conducted some additional experiments to demonstrate the efficiency of our framework. The  
 597 table below displays the GPU memory usage and the time required for a single training round. It  
 598 shows that our method is indeed more efficient than other similar condensation tasks. This is because  
 599 we reduce computational overhead by changing the optimization objective to the latent vector rather  
 600 than directly performing gradient descent on the graph data.

602 Table 5: Comparison of running time and GPU memory cost of different methods

603

DS	Consumption	DosCond	KiDD	Ours
NCI1	Time(s)	2.28	7.89	1.06
	GPU Memory(MB)	175.62	763.93	94.15
ogbg-molhiv	Time(s)	2.53	18.72	1.01
	GPU Memory(MB)	389.48	748.82	289.48

604

605

606

607 We also conducted some additional experiments to demonstrate the effectiveness of our framework.  
 608 The following table compares the performance of the graphs condensed using our method with that of  
 609 the original graphs. It shows the GPU memory usage and time required for a single round of training.  
 610 As shown in the table, our condensed dataset exhibits a significant performance advantage over the  
 611 original dataset, demonstrating the effectiveness of our method.

612 Table 6: Comparison of running time and GPU memory cost of original dataset and condensed dataset

613

DS	Consumption	Original	Condensed
ogbg-molhiv	Time(s)	0.6537	0.0021
	GPU Memory(MB)	1489.32	28.16
ogbg-molbbbp	Time(s)	0.5523	0.0020
	GPU Memory(MB)	1264.59	27.55

614

615

616

617 Then, we demonstrate the necessity of our method. Our GRCOND is designed for scenarios (e.g.,  
 618 hyperparameter tuning and architecture search that require a variety of GNN tests) involving multiple  
 619 model training processes using condensed datasets. It is essential to note that in these scenarios,  
 620 the one-time cost of condensation can be amortized across all downstream training tasks involved,  
 621 thereby effectively reducing the training time for subsequent tasks. The following shows the training  
 622 time of an example involving three training tasks on the same dataset ogbg-molhiv, using GCN, GAT,  
 623 and GIN, respectively. From this table, we can find that the condensation time (i.e., 1287.62s) is  
 624 indeed larger than the training time for each task using the original ogbg-molhiv dataset. However,  
 625 when considering all three tasks together, the overall training time using GRCOND (i.e., 1290.60s) is  
 626 significantly smaller than that of its counterpart (i.e., 2265.50s), demonstrating the superiority of our  
 627 approach in handling such a scenario.

628 Table 7: Time consumption in our scenarios

629

Scenario	Time (s)
Original Data + GCN	809.70
Original Data + GAT	765.75
Original Data + GIN	690.05
Total	2265.50
Condensation	1287.62
Condensed Data + GCN	1.05
Condensed Data + GAT	0.96
Condensed Data + GIN	0.97
Total	<b>1290.60</b>

648 B STRUCTURE PRESERVATION TEST  
649650 We quantitatively measure information preservation beyond accuracy. We test it through: the average  
651 degree of all graphs, the average number of triangles contained, and the average clustering coefficient.  
652 It can be seen that the small graphs we generated have a positive effect on preserving the degree of  
653 the original dataset.654  
655 Table 8: Various structural indicators between the original graphs and the condensed graphs  
656657  
658  
659  
660  
661

DS		avg. degree	avg. triangle	avg. clustering
NCI1	Original	4.3088	0.0462	0.0031
	Condensed	4.1041	0.1754	0.0205
PROTEINS	Original	7.4492	27.7438	0.5179
	Condensed	7.2509	47.875	0.5246

662  
663 We also validated the preservation of inter-graph relationships through multi-faceted evidence. We  
664 tested the cosine similarity of the embedding matrices of small graphs within the same class and the  
665 cosine similarity of the embedding matrices of different classes. We can observe a class distinction  
666 in the embedding matrix. Additionally, we tested the average number of triangles contained in each  
667 class of synthetic graphs.668  
669 Table 9: Various structural indicators between the graphs inter-class and intra-class  
670671  
672  
673  
674

	cosine_similarity	inter-class cosine_similarity	average triangles for class 0	average triangles for class 1
PROTEINS	0.9905	0.3245	8.2	3.4
NCI1	0.9864	0.4027	6.4	0.8